Extreme Self-Organization in Networks Constructed from Gene Expression Data

Himanshu Agrawal*

Department of Physics of Complex Systems, Weizmann Institute of Science, Rehovot 76100, Israel

We study networks constructed from gene expression data obtained from many types of cancers. The networks are constructed by connecting vertices that belong to each others' list of K nearest neighbors, with K being an *a priori* selected non-negative integer. We introduce an order parameter for characterizing the homogeneity of the networks. On minimizing the order parameter with respect to K, degree distribution of the networks shows power-law behavior in the tails with an exponent of unity. Analysis of the eigenvalue spectrum of the networks confirms the presence of the power-law and small-world behavior. We discuss the significance of these findings in the context of evolutionary biological processes.

Recent technical advancements have led to widespread use of gene chips for quantizing and monitoring the expression level of thousands of genes in parallel [1]. Presently, gene expression profiling has become an important tool for diagnosis and classification of diseases. It is being used extensively for identifying genes responsible for specific conditions, e.g., various cancers [2–6]. This is done using specialized clustering techniques developed in recent years [7–9]. Gene expression data can also be used for constructing networks of coexpressed and coregulated genes. Since proteins are the end product of gene expression, various types of protein networks [10] and gene networks are directly related. Consequently, networks of coregulated genes are expected to play a key role in biological processes. In this Letter, we outline results that show the relevance of these networks in evolutionary biological processes.

The volume of gene expression data obtained from typical experiments is enormous and contains information on expression of all the genes (presently almost 10 000 or more) marked on the chip. In any given condition, most of the genes are not important and do not express. As a result, before the expression data can be used for constructing networks, it requires extensive processing and filtering to eliminate uninformative genes. We skip these details here as they can be found with the source of the data [2–6] and elsewhere [7,8]. Henceforth, we assume that expression data for the selected set of informative genes is available in the form of a matrix having N rows and D columns. The rows represent the genes and the columns represent the samples/tissues. Furthermore, the expression values of each of the genes in this matrix are normalized to have a mean of zero and variance of unity across the samples.

The normalized expression levels are treated as coordinates of N genes, that form the vertices of the networks, in D dimensional space of samples. The network construction algorithm requires specification of the maximum number of neighbors K, $0 \leq K < N$, that a vertex can have. For a given K, the gene network is constructed using the following two step procedure. (i) For each vertex i, $i = 1, \ldots, N$, make a list L_i of its first K nearest neighbors. (ii) Connect all vertices i and j through an edge if $i \in L_j$ and $j \in L_i$, otherwise the vertices are not connected. This algorithm is derived from the K-nearest-neighbor parameter estimation method [11]. With some heuristic modifications, it had been used earlier in clustering analysis of various types of data [9]. We used the Euclidean norm as the distance measure for making the list of K nearest neighbors. Other distance measures can also be used. The results presented herein remain unaltered as long as the distance measure preserves the ordering of points obtained from the Euclidean measure.

For a given data set, the topological structure of networks generated by this algorithm depends strongly on the parameter K. For $K = 0$, the network consists of N isolated vertices, and for $K = N - 1$ each vertex is connected to all the other vertices. For most of the values of K, these networks have more than one connected component. As K increases, the connectivity of each vertex grows depending on its local environment. Vertices that lie close to each other tend to get mutually connected in preference to those lying farther away. Thus, all connected components in these networks have a small-world structure. Furthermore, for $K \gtrsim 3$ the networks have a giant connected component.

We analyzed networks constructed using several published gene expression data sets. To ensure that our results are not affected by possible bias of technology used for manufacturing the gene chips, we used expression data sets obtained using both oligonucleotide arrays [2–4] as well as cDNA microarrays [5,6]. For each network, we calculated $P(z)$ the probability of finding a vertex of degree z. $P(z)$ is normalized by N so that $\sum_z P(z) = 1$. Since these networks are small, $P(z)$ is very noisy. As a result, we calculated the cumulative probability distribution,

$$F(z) = \sum_{i=z}^{z_{max}} P(i), \qquad (1)$$

where z_{max} is the maximum degree in the network.

We also define a quantity $c = z + 1$. This quantity gives the size of the smallest cluster around a vertex with connectivity z that includes the vertex and its neighbors. It can also be considered as the size of a "droplet" that is formed by the vertex and its neighbors. Since the smallest and the largest values of z are 0 and z_{max}, the corresponding values for c become 1 and $c_{max} = 1 + z_{max}$, where c_{max} is the largest droplet size. The probability density $\tilde{P}(c)$ and cumulative distribution $\tilde{F}(c)$ corresponding to c are defined similarly to those for z. The linear relationship of c and z implies that $\tilde{P}(c) = P(z)$ and $\tilde{F}(c) = F(z)$. Outside the range of z and c, corresponding probability density functions are defined to be zero. Thus, $\tilde{F}(c)|_{c \leq 1} = F(z)|_{z \leq 0} = 1$ and $\tilde{F}(c)|_{c > c_{max}} = F(z)|_{z > z_{max}} = 0$.

The homogeneity of the networks can be characterized by a single order parameter. A suitable candidate for this is the area Λ enclosed by the $\tilde{F}(c)$ versus $c^\star = c/c_{max}$ curve between $c^\star = 0$ and 1. It takes values in the range 0 to 1 depending on the homogeneity of the network. Since c_{max} is finite and the values of c are evenly spaced, $\Lambda(K)$ is easily calculated using Trapezoidal rule and equals

$$c_{max}\Lambda(K) = \frac{1}{2}[1 - P(z_{max})] + \sum_{i=0}^{z_{max}} (i+1)P(i). \qquad (2)$$

The terms with factor of $1/2$ represent the area of strips at the boundary. Their contribution vanishes as the number of strips increases. It is zero if $P(z)$ is a delta function.

From Eq. (2), the value of $c_{max}\Lambda(K)$ is easily identified as the mean size $\bar{c} = 1 + \bar{z}$ of the droplets, where $\bar{z}$ is the average degree of vertices in the network. Thus, $\Lambda(K)$ is the average droplet size normalized with the size of the largest droplet in the network. It measures separation between the mean and maximum droplet sizes in the network and functions as an indicator of the overall behavior of $F(z)$ and $P(z)$. Very small values of $\Lambda(K)$ imply that $F(z)$ descends sharply from unity to almost zero at a small $z \ll z_{max}$ and becomes nearly flat with plateau stretching until z_{max}. The corresponding $P(z)$ has long tails with weight centered at small z. $\Lambda(K)$ close to unity implies that $F(z)$ stays nearly flat at unity for most of $z \leq z_{max}$ and descends sharply to zero at some $z \approx z_{max}$. In this case $P(z)$ is sharply peaked similar to a delta function near z_{max}. Intermediate values of $\Lambda(K)$ imply a decaying $F(z)$ corresponding to various forms of $P(z)$ including those that rise slowly to a peak and then decay slowly via sharply truncated power-law tails.

Figure 1 (Alon99) shows the behavior of $\Lambda(K)$ for networks constructed using colon cancer data of Alon *et al.* [2]. The figure shows that, as K is increased from 1 to $N - 1$, $\Lambda(K)$ initially decreases and attains a minimum at some value of $K = K_1$ (here $K_1 \approx 16$). The minimum is nearly flat and persists until $K = K_2$ (here $K_2 \approx 24$). As K
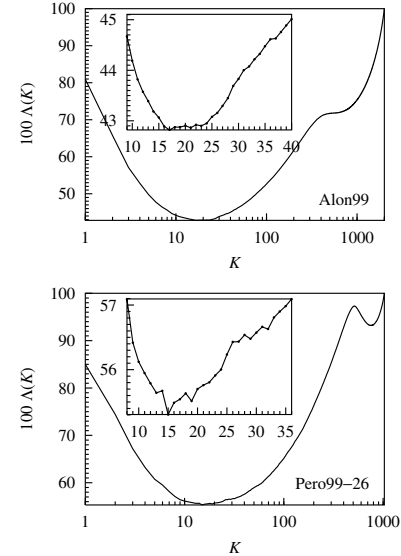

FIG. 1. Variation of $\Lambda(K)$ with K for networks constructed from colon cancer data of Alon *et al.* [2] and breast cancer data of Perou *et al.* [5]. The insets show a blowup of a small zone around the minima. The keys are as in [24].

is increased beyond K_2, $\Lambda(K)$ continues to increase, reaching its maximum value of 1 at $K = N - 1$. Figure 1 (Pero99-26) shows similar behavior of $\Lambda(K)$ in networks constructed using breast cancer data of Perou *et al.* [5] with a second minimum at $K \approx 3N/4$. The second minimum is usually a finite size effect. It can also occur if there is high inhomogeneity on length scales large compared to the nearest neighbors scale. It is very shallow compared to that between K_1 and K_2 because the probability density function corresponding to the size of "droplets" on larger length scales are sharper compared to $P(z)$ and also have smaller tails. The higher order minima, however, are not relevant. Behavior similar to that seen in Fig. 1 was observed in networks from several other gene expression data sets also [3,4,6].

The behavior of $\Lambda(K)$ divides the networks into three classes. (i) The networks corresponding to $1 \leq K < K_1$ have few connections between vertices but have high homogeneity. (ii) The networks for $K_1 \leq K \leq K_2$ are somewhat better connected and highly inhomogeneous. (iii) In the networks for $K_2 < K \leq N - 1$, the vertices have many connections and high homogeneity that increases with K.

Figure 2 shows the variation of the observed cumulative probability distribution $F(z)$ with the normalized degree $(z + 1)/(z_{max} + 1)$ in a wide range of values of K for networks constructed from many gene expression data sets [2–6]. It is clear from the figure that all the curves in the range $K_1 \leq K \leq K_2$ (solid circles) show a very good collapse, and thus good scaling, for all the data sets. This range of K houses the minimum of the order parameter and the corresponding networks are highly inhomogeneous with loosely connected vertices. The solid straight line passing through the tails of these
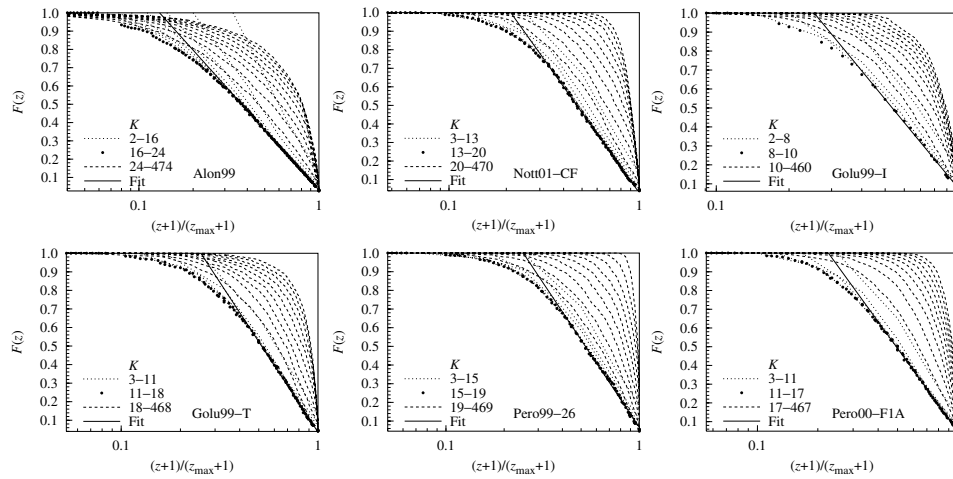
FIG. 2. Variation of cumulative probability distribution function $F(z)$ with normalized degree $(z + 1)/(z_{max} + 1)$ in networks constructed from several data sets. The keys are as in [24]. In the graphs, data for different types of networks are plotted using different line styles. Solid circles are used in the range of K corresponding to minima of $\Lambda(K)$. The straight solid line is least-square fit of the form given in Eq. (3) in the tails of $F(z)$. The curves drawn with dashed lines approach the solid circles as K increases (here, in steps of 2). The curves drawn with dotted lines go away from the solid circles as K increases (here, in steps of 50).

curves is a least-square fit of the form

$$F(z) = a - b \ln\left(\frac{z + 1}{z_{max} + 1}\right), \tag{3}$$

where a and b are the fit parameters. For the graphs shown in the figure, these parameters vary in the range $0.03 \le a \le 0.08$ and $0.47 \le b \le 0.71$ over all the data sets.

The extremely good fit of Eq. (3) in the tails of $F(z)$ seen in Fig. 2 implies that the corresponding probability density functions have a scale-free behavior of the form $P(z) \sim b(z + 1)^{-1}$ in the tails. The power law is seen in the range $0.35 \lesssim (z + 1)/(z_{max} + 1) \le 1$, i.e., in nearly 60% to 65% of the range of variation of vertex degree. As this range is small for observing heavy tailed distributions, we analyze the eigenvalue spectrum of the adjacency matrix of networks [12] to have another evidence of the scale-free character of the networks.

The spectral density $\rho(\lambda)$ of the eigenvalue spectrum of the adjacency matrix of networks

$$\rho(\lambda) = \frac{1}{N} \sum_{j=1}^{N} \delta(\lambda - \lambda_j), \tag{4}$$

where λ_j is the jth eigenvalue of the adjacency matrix, is a good indicator of the overall behavior of their degree

distribution $P(z)$ and topological structure. For random graphs having a giant connected component $\rho(\lambda)$ is known to converge to a semicircle following the Wigner's law [12]. Deviations from Wigner's law are seen for other cases. For the small-world networks $\rho(\lambda)$ shows a complex highly skewed structure with several blurred peaks [12]. For scale-free networks, the spectral density has a triangular shape with the central part lying above the semicircle [12].

Figure 3 shows the spectral density of networks constructed from colon cancer data of Alon *et al.* [2] for different values of K corresponding to the three zones of behavior of $\Lambda(K)$ seen previously. The figure shows that for small K the spectral density has an irregular shape with several blurred peaks and its bulk is confined below the semicircle. This is a characteristic of small-world networks [12]. As K is increased, the bulk portion starts assuming a triangular shape which is a little skewed for small K. The top portion of the triangle starts protruding above the semicircle as K crosses K_1. This is clear from the intermediate and high values of K in the figure. The triangular shape persists until K becomes almost equal to $N - 1$. At $K = N - 1$, the spectral density develops a delta function peak corresponding to $N - 1$ repeated
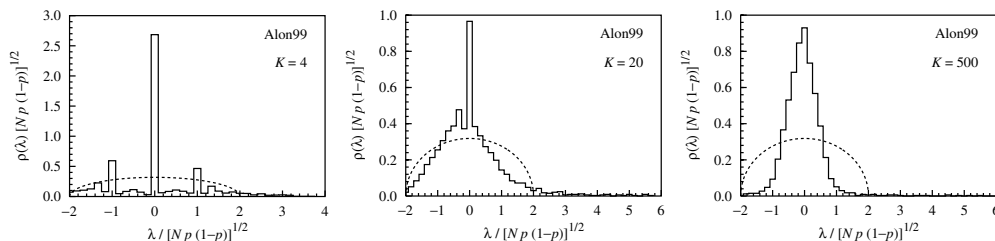

FIG. 3. Spectral density for networks constructed from colon cancer data of Alon *et al.* [2] for different values of K corresponding to the three zones of behavior of the order parameter $\Lambda(K)$ (see Fig. 1). p is the fraction of edges, out of the maximum possible $N(N - 1)/2$, present in the network. Semicircle corresponding to spectral density of random networks is drawn for comparison.

eigenvalues at $\lambda = -1$ and the largest eigenvalue is $\lambda_1 = N - 1$. This behavior of the spectral density was seen in all the other data sets also [3–6]. It confirms that these gene networks have small-world character and become scale free for $K \geq K_1$.

Presence of scale-free behavior indicates a high degree of self-organization in the system and is known to be a characteristic of natural systems [13]. It has been observed in several natural and artificial networks, e.g., power grid [14], the Internet [15], the World Wide Web [16], actor network [17], web of human sexual contacts [18], citation and collaboration networks [19], conceptual network of language [20], metabolic network [21], food web [22], and protein networks [10]. The exponents of the power laws observed earlier, however, were always more than unity. The gene networks studied here are first examples of biological networks showing scale-free behavior with exponent of unity.

The scale-free character of coexpressed gene networks means that these networks are extremely inhomogeneous and contain few genes that are very highly connected and a large number of genes with low connectivity. This implies that these networks contain large groups of coexpressed genes. As a result, the present study conclusively shows, using direct experimental data, that various types of cancers are a consequence of a malfunction of only a few genes that either regulate the expression of a large number of other genes or form the hubs of various crowded gene regulatory pathways functioning in the organism. It is known that disturbing such genes could be fatal for the organism [23], which also turns out to be the mechanism of origin of cancers. Identification of such genes and understanding their functionality under various conditions through which an organism can pass in its lifetime is directly relevant in the design of highly targeted drugs, among other possibilities.

The simultaneous presence of small-world and scale-free characters in these networks seems to be a perfect fit in the evolutionary scheme of biological systems. The high robustness displayed by biological systems is a consequence of the scale-free character of the associated networks. On the other hand, the fast reaction and rapid adaptability shown by biological systems can come only if the associated networks have a small-world character. This fits the structure of biological signaling system well because the chemical signaling employed at most places in biological systems, by its very nature, is very slow compared to, e.g., electrical signaling in neurons. Thus, for achieving fast message transmission, the associated networks must evolve to have small-world character.

*Electronic address: feagrawa@wicc.weizmann.ac.il

[1] E. S. Lander, Nature Genet. **21**, 3 (1999); D. Gerhold, T. Rushmore, and C. T. Caskey, Trends Biochem. Sci. **24**, 168 (1999).

[2] U. Alon *et al.*, Proc. Natl. Acad. Sci. U.S.A. **96**, 6745 (1999).

[3] D. A. Notterman, U. Alon, A. J. Sierk, and A. J. Levine, Cancer Res. **61**, 3124 (2001).

[4] T. R. Golub *et al.*, Science **286**, 531 (1999).

[5] C. M. Perou *et al.*, Proc. Natl. Acad. Sci. U.S.A. **96**, 9212 (1999).

[6] C. M. Perou *et al.*, Nature (London) **406**, 747 (2000).

[7] A. Brazma and J. Vilo, FEBS Lett. **480**, 17 (2000).

[8] M. B. Eisen, P. T. Spellman, P. O. Brown, and D. Botstein, Proc. Natl. Acad. Sci. U.S.A. **95**, 14863 (1998).

[9] M. Blatt, S. Wisemann, and E. Domany, Phys. Rev. Lett. **76**, 3251 (1998).

[10] H. Jeong *et al.*, Nature (London) **411**, 41 (2001); S. Maslov and K. Sneppen, Science **296**, 910 (2002).

[11] K. Fukunaga, *Introduction to Statistical Pattern Recognition* (Academic, San Diego, 1990).

[12] I. J. Farkas *et al.*, Phys. Rev. E **64**, 026704 (2001); K.-I. Goh, B. Kahng, and D. Kim, *ibid.* **64**, 051903 (2001).

[13] P. Bak, C. Tang, and K. Wiesenfeld, Phys. Rev. Lett. **59**, 381 (1987).

[14] D. J. Watts and S. H. Strogatz, Nature (London) **393**, 440 (1998).

[15] M. Faloutsos, P. Faloutsos, and C. Faloutsos, Comput. Commun. Rev. **29**, 251 (1999); R. Cohen, K. Erez, D. ben-Avraham, and S. Havlin, Phys. Rev. Lett. **85**, 4626 (2000).

[16] R. Albert, H. Jeong, and A.-L. Barabási, Nature (London) **401**, 130 (1999); B. A. Huberman and L. A. Adamic, *ibid.* **401**, 131 (1999).

[17] A.-L. Barabási, and R. Albert, Science **286**, 509 (1999).

[18] F. Liljeros *et al.*, Nature (London) **411**, 907 (2001).

[19] S. Redner, Eur. Phys. J. B **4**, 131 (1998); M. E. J. Newman, Proc. Natl. Acad. Sci. U.S.A. **98**, 404 (2001).

[20] A. E. Motter *et al.*, Phys. Rev. E **65**, 065102R (2002).

[21] H. Jeong *et al.*, Nature (London) **407**, 651 (2000).

[22] R. V. Solé and J. Montoya, Proc. R. Soc. London B **268**, 2039 (2001).

[23] J. Hasty and J. J. Collins, Nature (London) **411**, 30 (2001).

[24] Keys in the graphs are as follows. *Alon99*: 2000 genes in 62 samples from colon cancer data [2]. *Nott01-CF*: 1211 genes in 36 samples from colon adenocarcinoma data [3]. We used a nominal threshold of 20 and selected genes having standard deviation at least twice the mean standard deviation in $\log_2$-transformed expression data. *Golu99-I* (*Golu99-T*): 1049 (1030) genes in 34 (38) samples of the independent (training) set from acute leukemia data [4]. Genes were selected as for Nott01-CF using a nominal threshold of 215 (222). *Pero99-26*: 1030 genes in 26 samples in breast cancer data [5]. We selected genes that had good data in at least 20 samples and showed at least 2.5-fold variation above the median in at least two samples. *Pero00-F1A*: 1753 genes in 84 samples from breast cancer in supplementary data [6].